Mitochondrial Networking Protects β-Cells From Nutrient-Induced Apoptosis

Anthony J.A. Molina,[1] Jakob D. Wikstrom,[1,2] Linsey Stiles,[1,3] Guy Las,[1] Hibo Mohamed,[3] Alvaro Elorza,[1] Gil Walzer,[3] Gilad Twig,[1] Steve Katz,[3] Barbara E. Corkey,[1] and Orian S. Shirihai[1]

OBJECTIVE—Previous studies have reported that β-cell mitochondria exist as discrete organelles that exhibit heterogeneous bioenergetic capacity. To date, networking activity, and its role in mediating β-cell mitochondrial morphology and function, remains unclear. In this article, we investigate β-cell mitochondrial fusion and fission in detail and report alterations in response to various combinations of nutrients.

RESEARCH DESIGN AND METHODS—Using matrix-targeted photoactivatable green fluorescent protein, mitochondria were tagged and tracked in β-cells within intact islets, as isolated cells and as cell lines, revealing frequent fusion and fission events. Manipulations of key mitochondrial dynamics proteins OPA1, DRP1, and Fis1 were tested for their role in β-cell mitochondrial morphology. The combined effects of free fatty acid and glucose on β-cell survival, function, and mitochondrial morphology were explored with relation to alterations in fusion and fission capacity.

RESULTS—β-Cell mitochondria are constantly involved in fusion and fission activity that underlies the overall morphology of the organelle. We find that networking activity among mitochondria is capable of distributing a localized green fluorescent protein signal throughout an isolated β-cell, a β-cell within an islet, and an INS1 cell. Under noxious conditions, we find that β-cell mitochondria become fragmented and lose their ability to undergo fusion. Interestingly, manipulations that shift the dynamic balance to favor fusion are able to prevent mitochondrial fragmentation, maintain mitochondrial dynamics, and prevent apoptosis.

CONCLUSIONS—These data suggest that alterations in mitochondrial fusion and fission play a critical role in nutrient-induced β-cell apoptosis and may be involved in the pathophysiology of type 2 diabetes. ***Diabetes*** **58:2303–2315, 2009**

From the [1]Department of Molecular Medicine, Obesity Research Center, Boston University School of Medicine, Boston, Massachusetts; [2]The Wenner-Gren Institute, The Arrhenius Laboratories F3, Stockholm University, Stockholm, Sweden; and the [3]Department of Pharmacology and Experimental Therapeutics, Tufts University School of Medicine, Boston, Massachusetts.

Corresponding author: Orian S. Shirihai, orian.shirihai@tufts.edu.

Received 18 December 2006 and accepted 18 June 2009.

Published ahead of print at http://diabetes.diabetesjournals.org on 6 July 2009. DOI: 10.2337/db07-1781.

See accompanying commentary, p. 2185.

Mitochondria mediate β-cell responses to extracellular glucose by generating ATP and initiating a cascade of events culminating in the release of insulin. It is not surprising that β-cell mitochondria have become an important target for investigations into the etiology of type 2 diabetes. Mitochondria are highly dynamic organelles whose morphology is regulated by cycles of fusion and fission, collectively termed mitochondrial dynamics (1,2). Networks are formed when mitochondria undergo fusion events that cause the compartments of participating mitochondria to become continuous. As a result, the constituents of each network share solutes, metabolites, and proteins (3–5) as well as a transmembrane electrochemical gradient (1,6). The disruption of such networks has been shown to have a profound effect on the progression of cells to apoptosis, particularly in cases where reactive oxygen species (ROS) are involved (7). As such, mitochondrial networking is thought to be a potential defense mechanism allowing for the buffering of mitochondrial ROS and calcium overload (8,9).

Chronically elevated levels of glucose and fatty acid are thought to contribute to the progression of type 2 diabetes by adversely affecting β-cells and thereby causing a deterioration in insulin secretion (10). In vivo, a reduction in insulin gene expression due to reduced Pdx-1 binding has been observed in rats perifused with glucose and intralipids (11,12). In addition, exposure to high levels of glucose and/or free fatty acid has been shown to affect β-cell viability by inducing mitochondrial apoptosis and has been linked to ROS-induced mitochondrial calcium overload and damage (13). Recent studies indicate that nutrient-induced ROS increases subcellular mitochondrial membrane potential ($\Delta\Psi$mt) heterogeneity and fragmentation of the mitochondrial architecture (14,15). These findings suggest that mitochondrial fragmentation-defragmentation might play a role in the effects of noxious stimuli. Although the functional significance of these changes has not been studied in β-cells, studies of mitochondrial morphology in other cells have demonstrated that the ability of mitochondria to form networks influences both ROS and calcium handling (7–9).

Previous studies have reported that β-cell mitochondria form less elaborate network structures, compared with COS cells for example, and raise doubts on the existence of mitochondrial networking in these cells. Until now, technologies for examining and quantifying the ability of mitochondria to undergo fusion and fission were unavailable.

In this work, we show that the densely packed appearance of mitochondria in the β-cell represents the existence of multiple juxtaposed units that do not share continuous

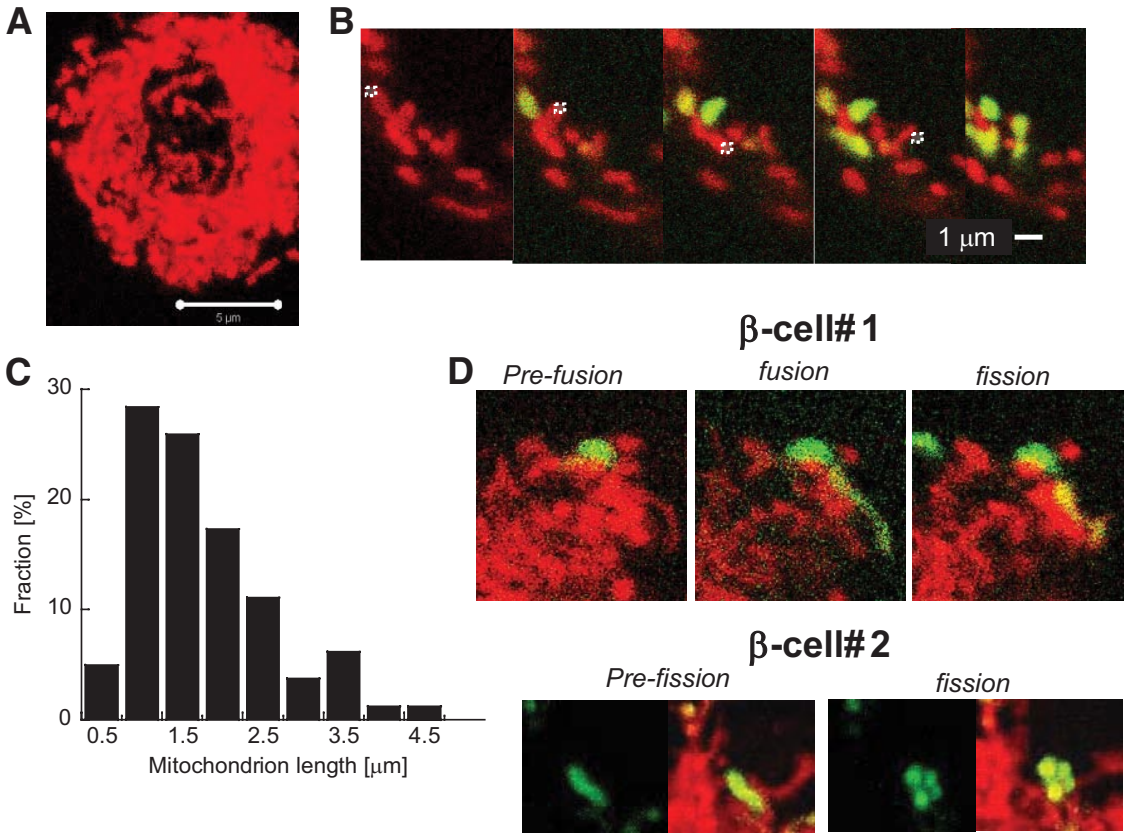

FIG. 1. Dissection of the mitochondrial web in primary β-cells using PAGFPmt. *A*: Projection of confocal images of a cell stained with TMRE. Note that mitochondria are densely packed in β-cells. *B*: Sequential 2-photon laser photoactivation of individual mitochondria. *C*: Summary of mitochondrial size distribution performed by 90 photoactivation steps in 9 cells. *D*: Tagging and tracking individual mitochondria in primary β-cells reveals fusion events (transfer of activated PAGFPmt to juxtaposed unlabeled mitochondria) that are then followed by fission events (separation of previously connected mitochondria). (A high-quality digital representation of this figure is available in the online issue.)

matrix lumen but do go through frequent fusion and fission events. We further demonstrate that mitochondrial dynamics are disrupted by exposure to the combination of high fat and glucose, gradually leading to the arrest of fusion activity and complete fragmentation of the mitochondrial architecture. Inhibiting mitochondrial fission preserved mitochondrial morphology and dynamics and prevented β-cell apoptosis.

RESEARCH DESIGN AND METHODS

Mitochondrial dynamics assays

Tagging and tracking mitochondria with matrix-targeted photoactivatable green fluorescent protein. Primary β-cells and INS1 cells were transfected with matrix-targeted photoactivatable green fluorescent protein (PAGFPmt) expressed under the insulin promoter and allowed to accumulate in the mitochondrial matrix for 48–72 h. Mitochondria were labeled with 7 nmol/l TMRE (tetramethylrhodamine-ethyl-ester-perchlorate; Invitrogen, Eugene, OR) for 45 min prior to imaging to allow visualization. The transition to active green fluorescent protein (GFP) was achieved by photoisomerization using 2-photon laser (750 nm) excitation to give a 375 nm photon equivalence at the focal plane. This allowed for selective activation of regions <0.5 μm^2 (Zeiss LSM510) or >4 μm^2 (Leica TCS SP2). In the absence of photoactivation, PAGFPmt protein molecules remained stable in preactivated form. The presence of preactivated PAGFPmt was detected using high-intensity excitation at 488 nm in combination with a fully opened collection pinhole.

Whole-cell mitochondrial fusion assay. We used the dilution of PAGFPmt into the mitochondrial web as an index for mitochondrial fusion (16). A region of interest (ROI) occupying 10–15% of the cell in one confocal section was activated using a 2-photon laser (350 nm equivalence at the focal plane). The dilution of activated PAGFPmt within the mitochondrial web was assessed by repeatedly scanning the entire cell volume (six confocal *z*-axis section projection) at 3- to 10-min time intervals for 50 min.

Image analysis. Quantification of fusion was performed using Metamorph (Molecular Devices, Sunnyvale, CA) by measuring the average fluorescence intensity (FI) of the mitochondria that became PAGFPmt positive based on a fixed threshold. The GFP FI values of PAGFPmt dilution were normalized to the GFP FI value immediately after photoactivation and then fitted to a hyperbolic function: $F(t) = 1 - F_{plateau} \times t/(t + T_{50})$. F and $F_{plateau}$ denote FI at time t and in the plateau phase. T_{50} denotes the time interval to a 50% decrease in normalized GFP FI ($[1 - F_{plateau}]/2$). All fitting procedures and statistical tests were conducted using Kaleida-Graph software (Synergy Software, Reading, PA). Paired Student's t tests were performed to calculate statistical significance.

Prior to measuring FI, we used an integrated morphometry analysis function designed for these experiments to extract PAGFPmt-positive structures that were larger than 10 pixels. These areas were interpreted to be mitochondria, and their TMRE FIs were recorded. This procedure enabled the selection of mitochondrial structures using very low threshold levels in the green channel (~10% of the image average intensity), assuring that >90% of the mitochondrial pixels were included for analysis. To set the threshold level, a test-threshold function first measured the average green FI of the mitochondria. The lower (inclusive) threshold was set at two-thirds of this average. Prior to analysis, all images were scanned to verify that all intensity measurements were below saturation; therefore, an upper threshold was not necessary.

RESULTS

Characterizing mitochondrial architecture and dynamics in β-cells. Primary β-cells isolated from mice exhibit dense mitochondrial architecture as revealed by confocal microscopy. A three-dimensional reconstruction of mitochondria within an entire β-cell has been projected onto a single plain to illustrate the density of these organelles (Fig. 1*A*). This morphology suggests the presence of either large continuous networks throughout the

cell or, alternatively, small discrete networks juxtaposed with one another. To decipher this complex architecture to its individual components, we double labeled the mitochondrial web with TMRE and PAGFPmt (6). Because individual mitochondria are often in apposition with one another, tagging individual mitochondria with PAGFPmt targeted to the matrix allows morphological and biophysical studies of mitochondria within a complex web. In addition, this methodology takes into account organellar movement and mitochondrial dynamics that continuously change the mitochondrion's size, shape, and location (6). With adenoviral delivery, PAGFPmt is expressed in all β-cell mitochondria but remains in its inactive form (nonfluorescent).

Precise (0.5 μm^2) photoactivation of PAGFPmt molecules was achieved using a 2-photon laser. Equilibration of activated PAGFPmt was immediate and revealed the boundaries of matrix continuity of individual mitochondria. Figure 1*B* shows five sequential photoactivations revealing the boundaries of multiple individual mitochondrial networks in a mouse β-cell. Whereas TMRE staining may show continuous mitochondrial structures, the spread of matrix PAGFPmt is limited to short segments, indicating that these segments do not form a continuous lumen. In 90 photoactivation events performed in nine different cells, we found that most (>95%) individual networks are rod-like in shape with 76% exhibiting a length <2 μm (Fig. 1*C*). A series of control studies confirmed that laser intensity was kept at levels that did not affect mitochondrial function or morphology. These included time-lapse studies of ΔΨmt in cells exposed to sequential laser scanning and dose-response studies with the 2-photon laser (experiments are described in an online appendix at http://diabetes.diabetesjournals.org/cgi/content/full/db07-1781/DC1 and in ref. 6). The small network size of β-cell mitochondria raises the possibility that mitochondrial fusion is absent in these cells or, alternatively, that fusion events are transient and brief. To address this issue, PAGFPmt was used to detect mitochondrial fusion events. Fusion events were identified by the transfer of PAGFPmt from a labeled mitochondria to a previously unlabeled one when the two came in contact as shown in Fig. 1*D*. Fusion events were commonly followed by fission (11 of 12 events) in a manner that reverted to prefusion size and morphology of the involved mitochondria. A similar pattern was observed in INS1 cells (supplemental Fig. S3 of the online appendix).

We undertook a series of experiments designed to manipulate the balance between fusion and fission to assess the consequence on mitochondrial architecture in primary and clonal β-cells. Of particular interest is the fusion protein OPA1 because transcriptom databases suggest its expression levels in the β-cell is uniquely high (www.t1dbase.org). To test the significance of OPA1 in modulating β-cell mitochondrial architecture, we overexpressed the protein by adenoviral transduction. Overexpression of OPA1 in primary β-cells caused mitochondria to fragment into even smaller units (Fig. 2*A*). In INS1 cells, transduction with the same number of OPA1 adenoviral particles caused mild overexpression and increased density in mitochondrial architecture. Increasing the amount of virus further increased the expression level and led to fragmentation of the mitochondrial network (Fig. 2*B*). These findings suggest that the increased degree of fusion may promote elongation; however, further increases in OPA1 levels can lead to fragmentation. GFP infections were performed to control for potential effects of viral transduction and normalized so that cells were exposed to the same number of viral particles. We found that expression of GFP did not affect mitochondrial morphology in any of the experiments performed.

An alternative approach to examining the consequences of a pro-fusion state is to prevent fission. We found that manipulating the pro-fission protein DRP1 also caused dramatic changes in mitochondrial architecture. Disruption of fission in primary β-cells by overexpressing dominant negative (DN) DRP1 resulted in swelling of the mitochondria (Fig. 2*C*). In INS cells, similar treatment with DN DRP1 caused elongation and swelling of the mitochondrial networks (Fig. 2*D*).

The overall rate of mitochondrial fusion activity within an isolated β-cell was assessed by photoactivating a subpopulation of mitochondria and monitoring the spread as well as the dilution of active PAGFPmt throughout the rest of the cell's mitochondria (Fig. 3*A* and supplemental movie *A*). The gradual spread of PAGFPmt signal to other parts of the β-cell, which were not photoactivated, is accompanied by dilution of PAGFPmt (Fig. 3*A* and *B*). As a result, the average PAGFPmt fluorescence intensity in mitochondria that contain photoactivated PAGFPmt gradually decreases as long as the process of spreading is in progress. When spreading of PAGFPmt reached equilibrium, FI was significantly lower and remained stable.

To rule out the possibility that decay in PAGFPmt FI was the result of either nonspecific leak of activated PAGFPmt from tagged mitochondria or bleaching of PAGFP by the laser, two experiments were conducted: GFP FI was measured over time *1*) in individual mitochondria that did not engage in fusion events and *2*) in the presence of FCCP, a mitochondrial inner membrane uncoupler that collapses $\Delta\psi_m$ and arrests mitochondrial dynamics. In both experiments GFP FI remained unchanged and stable over a period of 20 min, indicating a negligible component of nonspecific PAGFPmt leak or laser-induced bleach (see "mitochondrial fusion assay" in supplemental material).

Individual β-cells within an islet were tested for mitochondrial fusion activity using PAGFPmt that is under the insulin promoter (Fig. 3*C*). We found that fusion activity is functional and comparable with that in isolated β-cells. Interestingly, there is greater heterogeneity in the overall fusion activity among individual cells within intact islets exhibiting varied rates of GFP dilution (Fig. 3*D*). This is evident when comparing the standard deviations of GFP intensity at equilibrium.

Nutrient effects on primary β-cell mitochondria. Exposure to increased levels of glucose and fatty acids has been shown to compromise β-cell function and viability (10). Incubation in 20 mmol/l glucose along with the fatty acid palmitate (0.4 mmol/l complexed with 0.5% BSA) for 48 h resulted in fragmentation of mitochondrial morphology and inhibition of mitochondrial dynamics in β-cells within mouse islets (Fig. 3E), compared with controls in Fig. 3. The mitochondrial fusion capability of β-cells decreased significantly under HFG (20 mmol/l glucose and 0.4 mmol/l palmitate) which was revealed by the decreased ability of cells to dilute the GFP signal 2 h after photoactivation (Fig. 3*F*).

Individual and combined effects of fatty acids and high glucose in INS1 cells. El Assaad et al. (10) showed that in INS1 cells, exposure to 20 mmol/l glucose and >0.2 mmol/l palmitate for 24 h leads to apoptosis and that

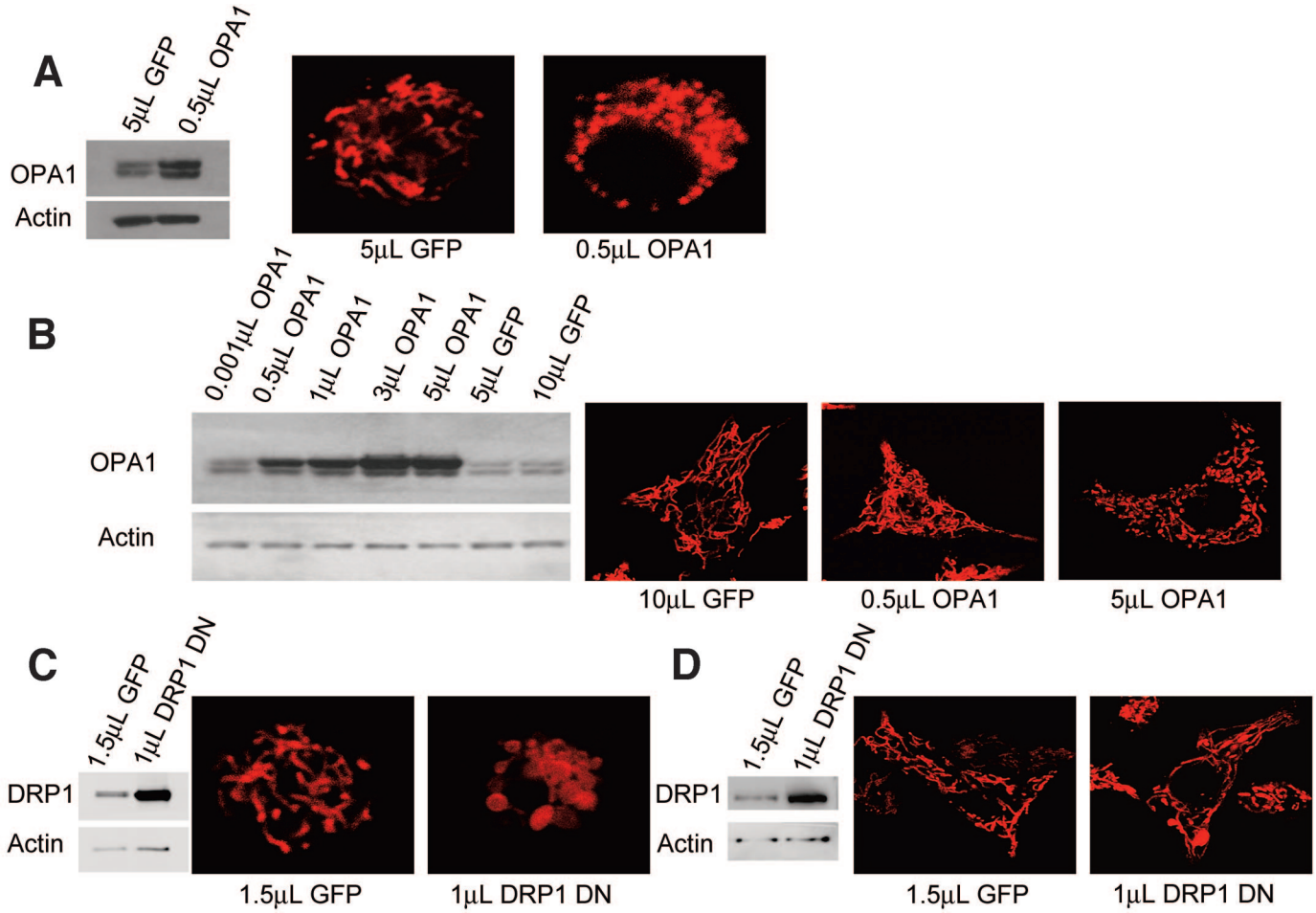

FIG. 2. Mitochondrial morphology is modulated by mitochondrial fusion and fission proteins in β-cells. *A*: In primary β-cells, overexpression of the fusion protein OPA1 leads to mitochondrial fragmentation. Overexpression was achieved by adenoviral transduction of GFP or OPA1 at equal concentrations of viral particles. *B*: Level of OPA1 overexpression in INS1 cells was controlled by the dose of viral particles used. Mild overexpression causes mitochondria to take on a dense and elaborate morphology compared with controls. Further increases in OPA1 overexpression levels resulted in mitochondrial fragmentation. *C*: In primary β-cells, overexpression of DN DRP1 to reduce mitochondrial fission leads to mitochondrial swelling. *D*: In INS1 cells, overexpression of DN DRP1 leads to network superfusion and a limited amount of mitochondrial swelling. The number and concentration of viral particles used in *A*, *C*, and *D* was identical. (A high-quality digital representation of this figure is available in the online issue.)

caspase inhibitors do not rescue the cells from death (10). We used confocal imaging of mitochondria to examine alterations in morphology caused by alterations in nutrient level (Fig. 4*A*). Cells were assessed visually, and those possessing >50% punctate mitochondria were considered fragmented. Exposure to 0.4 mmol/l palmitate in combination with 5, 11, or 20 mmol/l glucose (HFG) caused fragmentation in 40, 75, and 88% of cells after 4 h and in 51, 61, and 79% of cells after 24 h, respectively (Fig. 4*A*). Only 16 and 28% of cells exposed to 20 mmol/l glucose without palmitate for 4 and 24 h, respectively, exhibited fragmented mitochondrial architecture. These data indicate that increasing levels of glucose in the presence of palmitate is deleterious to mitochondrial architecture. However, increased glucose alone has a minor effect on mitochondrial fragmentation.

HFG-induced fragmentation is accompanied by reduced mitochondrial fusion in INS1 cells. To determine the effect of HFG on mitochondrial fusion, we measured the spread of PAGFPmt across the mitochondrial population by quantifying its dilution. As shown in Fig. 4*B* and *C*, 24-h HFG–treated cells with fragmented mitochondria failed to share the activated PAGFPmt. GFP FI remained unchanged ($n = 5$; $P = 0.46$) in HFG-treated cells 50 min after photoactivation, compared with a significant decrease observed in control cells ($n = 6$; $P < 0.001$). Interestingly, 4-h exposure to HFG was sufficient to impair fusion ability (Fig. 4*E*). These data reveal that fusion is compromised in fragmented mitochondria observed under HFG and that the reduction in fusion activity is measurable long before apoptosis. Fusion activity was also monitored in cells exposed to palmitate or varying levels of glucose for 24 h. We found that similar to HFG, HF (11 mmol/l glucose and 0.4 mmol/l palmitate) inhibits the mitochondrial fusion ability, whereas HG (20 mmol/l glucose) and HFLG (5 mmol/l glucose and 0.4 mmol/l palmitate) leave fusion intact (Fig. 4*D*).

We sought to determine whether the observed decrease in fusion activity is specific to HFG-induced toxicity as opposed to a physiological response to glucose challenge that is part of the glucose-stimulated insulin secretion (GSIS) cascade (Fig. 4*E*). INS1 cells were kept at 2 mmol/l glucose for 2 h before exposure to two different stimulatory conditions: 8 and 15 mmol/l glucose. In these experiments glucose concentration was switched immediately after a group of mitochondria had been labeled, and thus

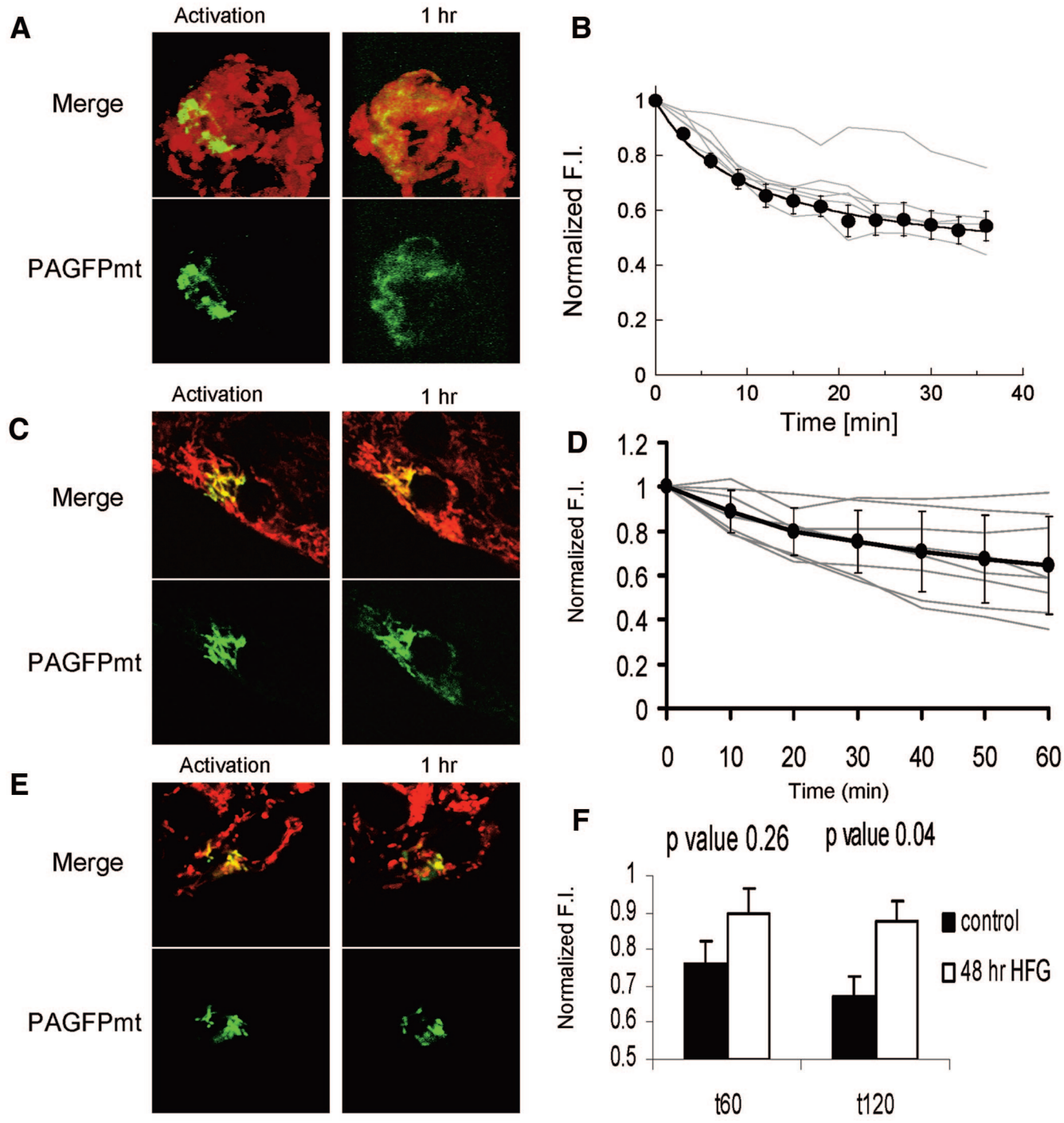

FIG. 3. Mitochondrial fusion and fission in primary β-cells. *A*: Fusion of the photoactivated fraction (~10%) with the rest of the mitochondrial web dilutes activated PAGFPmt and leads to a reduction in fluorescence intensity. A plateau is reached within ~40 min. Images are representative Z-projections. *B*: Dilution of GFP FI is shown for individual cells (n = 6; gray lines) and their average ± SE (●). The average dilution values were fitted (R = 0.99) to a hyperbolic function yielding T_{50} of 12.1 min. *C* and *D*: β-Cells within an intact islet also exhibit mitochondrial dynamics as revealed by the diffusion of the activated PAGFPmt signal. (See RESEARCH DESIGN AND METHODS and supplemental material for imaging and image analysis methodology). *E*: Fusion activity in primary β-cells is reduced after 24 h in HFG media. Images taken during the assay show that the number of PAGFPmt-positive mitochondria and the FI of PAGFPmt remained unchanged. *F*: Quantitative summary of PAGFPmt dilution shown 60 and 120 min after photoactivation. The HFG-treated cells possess significantly brighter GFP intensity (P = 0.04) than controls, indicating reduced mitochondrial fusion activity. (A high-quality digital representation of this figure is available in the online issue.)

the effect of acute glucose challenge on fusion activity was tested within the first 30 min of the exposure. We find that neither of these conditions resulted in statistically significant changes in mitochondrial fusion capacity of the INS1 cells when compared with 2 mmol/l glucose. These data suggest that mitochondrial fragmentation and loss of fusion capacity are specific to noxious external stimuli and are not altered during normal β-cell function.

Role of mitochondrial fission machinery in the response to HFG. We hypothesized that the fragmented mitochondrial morphology that accompanies HFG is mediated by alterations in the balance between fusion and

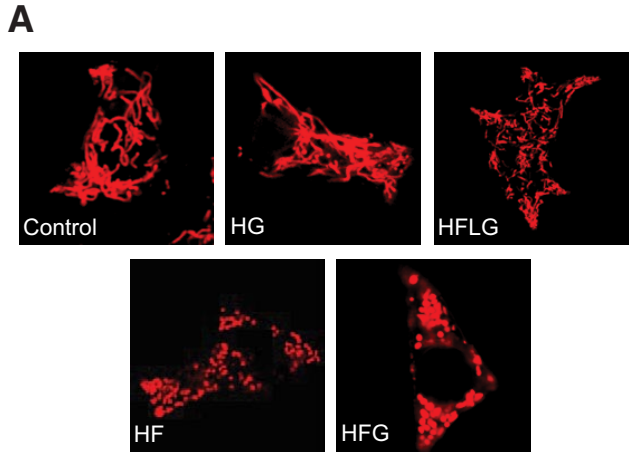

Condition	N	% Fragmented
Control (4 hours)	51	27
HG (4 hours)	54	16
HFLG (4 hours)	82	40
HF (4 hours)	51	75
HFG (4 hours)	51	88
Control (24 hours)	95	13
HG (24 hours)	149	28
HFLG (24 hours)	72	52
HF (24 hours)	147	61
HFG (24 hours)	138	79

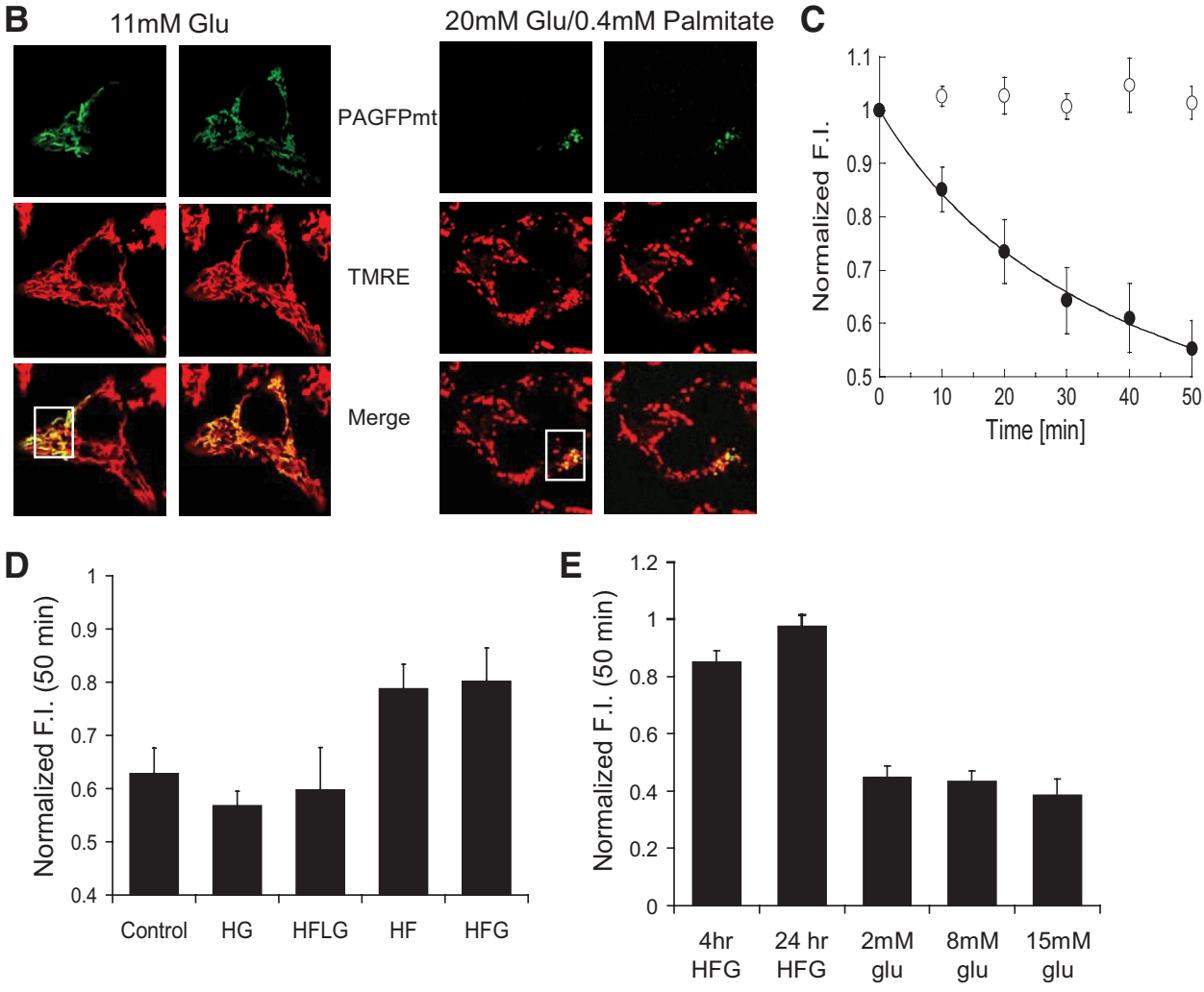

FIG. 4. Culturing INS1 cells in media with high levels of fatty acids and glucose impairs mitochondrial morphology and dynamics. *A*: Confocal images of INS1 cells stained with TMRE after 24 h in control (11 mmol/l glucose), HG (20 mmol/l glucose), HFLG (5 mmol/l glucose and 0.4 mmol/l palmitate), HF (11 mmol/l glucose and 0.4 mmol/l palmitate), and HFG (20 mmol/l glucose and 0.4 mmol/l palmitate) media. HF and HFG induce mitochondrial fragmentation within 4 h as opposed to incubation with control, HFLG, and HG media, which induce little or no effect on morphology. Cells possessing >50% fragmented mitochondria were considered fragmented. *B*: Assessment of mitochondrial fusion activity using the same approach as in Fig. 3. A group of mitochondria were labeled using a 2-photon laser (□, *inset*). Through fusion events, photoactivated GFP distributed itself throughout the mitochondrial network within 50 min in cells treated with control media. Redistribution is accompanied by dilution of the photoactivated form of PAGFPmt, revealed by the decreased PAGFPmt FI. In cells pretreated with HFG for 24 h (*right panel*), the activated PAGFPmt remained segregated in the mitochondria where it was initially photoactivated; dilution does not occur and PAGFP FI

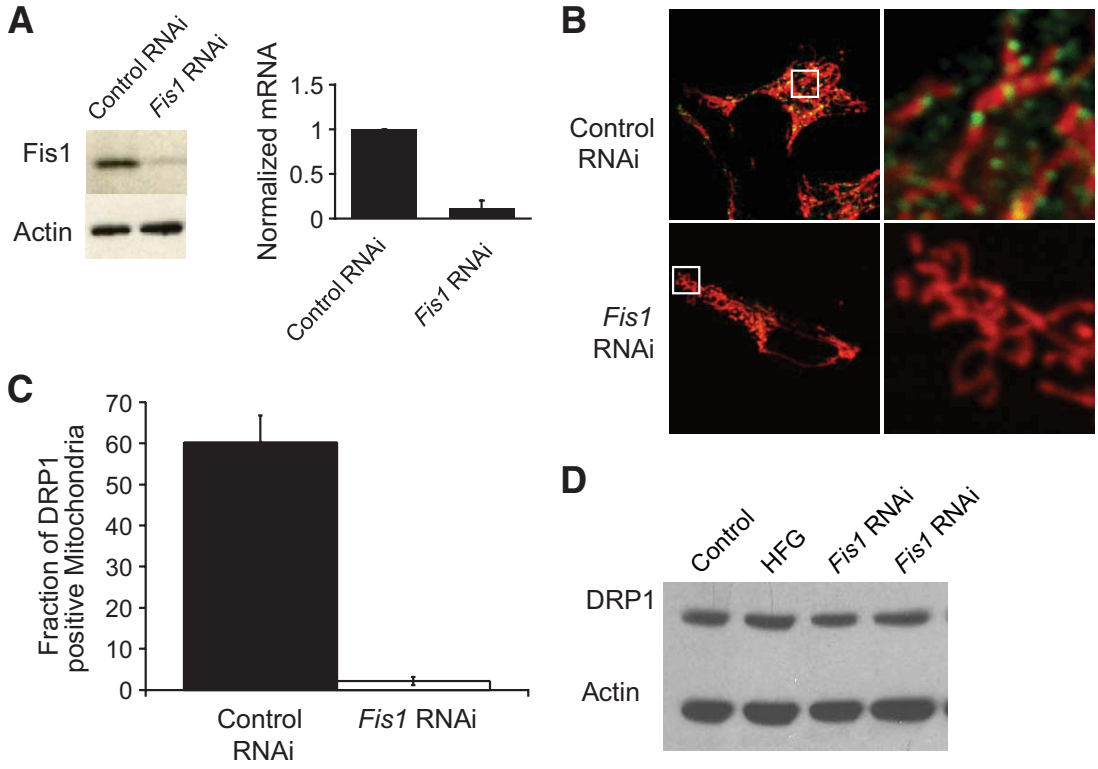

FIG. 5. Recruitment of DRP1 to mitochondria under HFG is prevented by Fis1 knockdown. *A*: Western blot and qPCR analysis of INS1 cells infected with control or *Fis1* RNAi lentivirus. Fis1 protein level was reduced by 80–90%, and RNA transcripts were reduced by an average of ~83% ($n = 5$). *B*: INS1 cells expressing mitochondrially targeted DsRed were stained for DRP1 (green). After 3.5 h of HFG incubation, DRP1 puncta are abundant in the control RNAi cells but not in the *Fis1* RNAi cells. *C*: Quantification of DRP1 recruitment to mitochondria after 3.5-h exposure to HFG ($n = 7$ for each group). *D*: Western blot analysis indicates that the changes in DRP1 recruitment observed were not due to changes in DRP1 expression levels because these remained the same in all the treatments tested. (A high-quality digital representation of this figure is available in the online issue.)

fission processes. Because these processes typically occur in a 1:1 ratio (17), our hypothesis predicts that reduction in fusion activity may be counteracted by reduced fission. We chose to reduce the expression levels of Fis1 because it plays a rate-limiting function in the recruitment of DRP1.

We were able to inhibit the expression of Fis1 using a shRNA sequence described previously (18,19). Protein levels are reduced by ~90%, and RNA transcripts are reduced by an average of 83% (n = 5; Fig. 5*A*). It is notable that in INS1 cells the knockdown of Fis1 does not cause noticeable alterations in mitochondrial morphology (supplemental Figs. S5 and S6A) (17,20).

We have previously reported that β-cell mitochondria exist as individual units that can exhibit differences in membrane potential (14). With exposure to HFG, membrane potential heterogeneity increased due to the appearance of depolarized mitochondria. Interestingly, the loss of fission ability by Fis1 knockdown or by the expression of DRP1 DN did not prevent the increase in membrane potential heterogeneity (supplemental Fig. S6).

To determine the efficiency of Fis1 knockdown on the inhibition of fission machinery, we tested its effect on DRP1 recruitment to fission sites (Fig. 5*B*). Colocalization of DRP1 puncta to mitochondria was visualized and quantified by immunofluorescence in control and lentivirally transduced *Fis1* RNAi INS1 cells exposed to 4 h of HFG. This time period corresponds to the duration required to achieve full fragmentation of the mitochondrial web without apoptosis (Fig. 4*A*). With Fis1 knockdown, the formation of DRP1 puncta along mitochondria is prevented. Control cells transduced with empty vector exhibited numerous DRP1-positive puncta along every mitochondrial network after 4 h of HFG. Colocalization of DRP1 puncta with mitochondria was significantly higher in the empty vector control group compared with *Fis1* RNAi ($P < 0.001$; Fig. 5*C*). A Western blot was performed to test whether HFG, Fis1 knockdown, or a combination of both affected the expression of DRP1. We find that DRP1 expression levels did not change under these conditions, thereby supporting that Fis1 knockdown and HFG affected puncta formation alone without altering DRP1 expression (Fig. 5*D*). In addition, immunostaining for DRP1 in control INS1 cells exposed to HFG for 4 h revealed the same

remains high. *C*: Quantitative summary of PAGFPmt dilution within the mitochondrial population after 24 h of HFG. ○, Cells exposed to HFG for 24 h; ●, cells incubated in normal growth media for the same amount of time. Average GFP dilution values were fitted ($R = 0.99$) to a hyperbolic function yielding T_{50} of 10.1 min only for the normal media group. *D*: Mitochondrial fusion activity, measured by the ability to dilute PAGFPmt after 50 min. Histogram shows steady-state values of GFP FI obtained 50 min after photoactivation, when the PAGFPmt dilution reached equilibrium. HFG- and HF-treated cells show reduced fusion activity compared with control and HFLG- and HG-treated cells ($P < 0.05$). *E*: A 4-h HFG treatment is sufficient to reduce the fusion activity of INS1 cell mitochondria to levels similar to those found with 24-h HFG treatment. Mitochondrial fusion activity is not affected by 30-min challenge with 8 and 15 mmol/l glucose. Glucose media was changed from 2 to 8 or 15 mmol/l 10 min prior to photoactivation. The plateau GFP FI level after 50 min is similar to that of the INS1 cells that remained in 2 mmol/l glucose. (A high-quality digital representation of this figure is available in the online issue.)

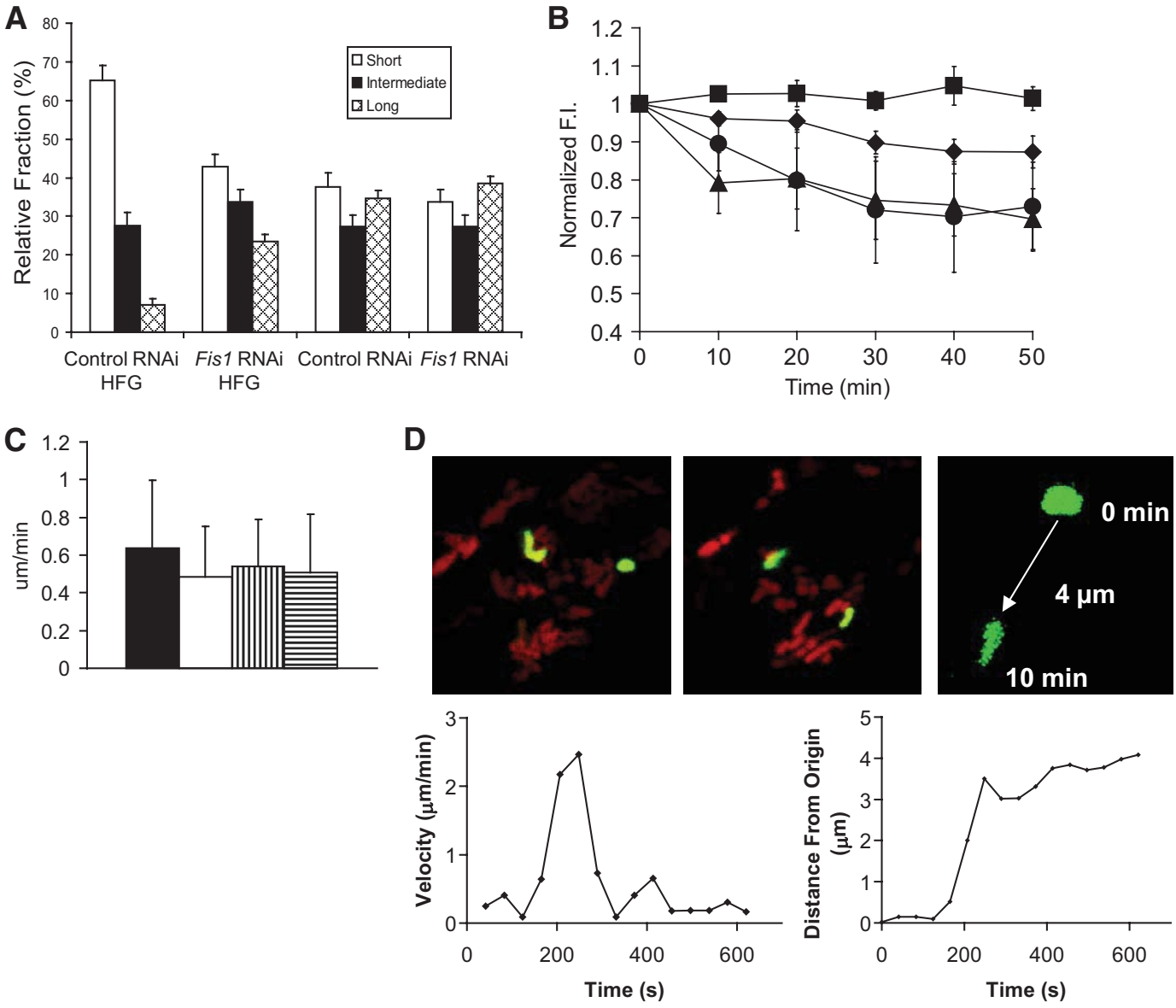

FIG. 6. ***Fis1*** **RNAi restores mitochondrial morphology and dynamics under HFG in INS1 cells.** ***A*****: Mitochondrial morphometry. Mitochondria were classified according to AR into short (AR <2), intermediate, (2<AR<4), and long (AR >4) length (*n* = 8 cells per group).** ***B*****: Whole-cell mitochondrial fusion assays (PAGFPmt dilution) in** ***Fis1*** **RNAi INS1 cells exposed to HFG for 24 h (▲). A hyperbolic fitting yielded T_{50} = 7.6 min.** ***Fis1*** **RNAi cells not exposed to HFG are also plotted (♦). Values of control RNAi cells with and without HFG treatment were imported from Fig. 3*C* (■ and ○, respectively).** ***C*****: Mitochondrial movement was calculated by measuring the velocity of single mitochondria over time. Velocities are not significantly different between groups (*P* >0.05). Control RNAi with and without HFG treatment are represented by ■ and □, respectively.** ***Fis1*** **RNAi cells with and without HFG treatment are represented by ▥ and ▤, respectively.** ***D*****: Confocal images demonstrating mitochondrial movement analysis. Images at time 0 and 10 min are portrayed. The last image zooms to one mitochondrion and the movement over 10 min is depicted, in this case 4 µm over 10 min. The velocity over time is plotted and indicates a peak around 250 s. When the distance from the origin is plotted over time, it is evident that mitochondria do not move at a constant speed. (A high-quality digital representation of this figure is available in the online issue.)**

staining pattern as cells not exposed to HFG (supplemental Fig. S4).

Effect of Fis1 on mitochondrial fragmentation, mitochondrial dynamics, and movement velocity under HFG. Inhibition of DRP1 recruitment to mitochondria suggests that *Fis1* shRNA can effectively prevent mitochondrial fission in β-cells. We next determined whether Fis1 knockdown can prevent HFG-induced fragmentation by performing morphometrical analysis of mitochondrial structures in INS1 cells infected with *Fis1* shRNA and control shRNA viruses.

INS1 cells infected with control virus were cultured in either 11 mmol/l (normal growth/culture conditions) glucose or with 20 mmol/l glucose and 0.4 mmol/l palmitate for 24 h and stained with TMRE. Under HFG, we observed a change from elongated and elaborate networks to fragmented and punctate mitochondria (Fig. 6*A*). The aspect ratio (AR) of all mitochondria in each cell was calculated by measuring the length and width of best fit ellipses (see RESEARCH DESIGN AND METHODS; an AR of 4 represents a mitochondrion that is four times longer than it is wide). Organelles were classified according to AR values into those with short (AR ≤2), intermediate (2<AR≤4), and long (AR >4) morphology. HFG treatment reduced the fraction of long mitochondria fivefold and doubled the fraction of short mitochondria. Fis1 knockdown signifi-

cantly reduced the appearance of short mitochondria under HFG treatment. Furthermore, the number of long mitochondria was tripled. It is notable that *Fis1* RNAi alone did not alter the distribution of short, intermediate, and long mitochondria within a cell's mitochondrial population (Fig. 6*A*).

In addition to rescuing mitochondrial architecture, Fis1 knockdown also preserved the capability of mitochondria to fuse after 24-h HFG treatment. Whereas cells transduced with control lentiviral treatment were unable to diffuse GFP after HFG treatment, those transduced with *Fis1* RNAi lentivirus reduced GFP intensity by 31%, similar to control cells not treated with HFG that exhibited a 29% decrease in GFP intensity (Fig. 6*B*). Fis1 knockdown alone also caused a mild decrease in mitochondrial fusion ability, exhibiting a 14% intensity decrease after 50 min. This result suggests the importance of fission in mitochondrial dynamics. It is reasonable to infer that with decreased fission, mitochondrial dynamics may occur more slowly although the network morphology remains unchanged.

It is possible that alterations in mitochondrial dynamics that we report are caused by changes in mitochondrial movement or velocity. Using PAGFPmt and time-lapse imaging of Z-stacks, we were able to tag and quantify the velocity of mitochondria under a variety of conditions. We found that the velocity (μm/min) of mitochondria remains unchanged by HFG or Fis1 knockdown compared with controls (Fig. 6*C*). *P* values are >0.05 when comparing the effects of HFG and *Fis1* RNAi. Figure 6*D* depicts two mitochondria tagged and tracked for velocity. Note that one mitochondrion remains relatively immobile during the time of tracking, whereas the other (shown in greater detail) moves 4 μm over the 10-min period. We find that mitochondrial movement does not occur in a smooth linear fashion. Rather, we observe spikes in the rate of movement over time similar to what has been reported in other cell types (21). This is also evident when looking at the distance from the origin at various time points. In the example provided, the maximal distance from the origin is reached between 120–250 s.

Reduced Fis1 expression by RNAi protects against HFG-induced apoptosis. Previous studies have demonstrated that HFG induces β-cell apoptosis (10). We proceeded to examine the effect of *Fis1* RNAi on HFG-induced apoptosis. Control and *Fis1* RNAi INS1 cells were exposed to HFG for 24 h and tested for various molecular markers of apoptosis (Fig. 7*A–C*). Immunostaining for cleaved caspase-3 as well as the 17 kDa and 19 kDa proapoptotic active forms of caspase-3 revealed a reduction back to basal levels in the *Fis1* RNAi cells exposed to HFG. The percentage of control INS1 cells exhibiting staining for cleaved caspase-3 staining (78 ± 4%) was significantly greater compared with *Fis1* RNAi–treated cells (25 ± 3%) when exposed to 24-h HFG (Fig. 7*A*). Similar results were found when apoptosis was analyzed using transferase-mediated dUTP nick-end labeling staining (Fig. 7*B*). Fis1 knockdown cells did not possess the dark nuclear staining, indicating that they are not undergoing apoptosis. Consistent with the immunofluoresence and TUNEL data, fluorescence-activated cell sorter analysis using annexin V, another apoptotic marker, revealed a dramatic reduction in apoptotic cells in *Fis1* RNAi–infected cells exposed to HFG (Fig. 7*C*).

Phosphorylated Akt (pAkt) has been shown to protect a variety of cell types, including β-cells, from apoptosis through the inhibition of proapoptotic proteins including BAD and caspase-9 (22,23). Previous studies have found that β-cell survival under elevated glucose or fatty acid is dependent on Akt phosphorylation (24–26). To determine whether *Fis1* RNAi was upstream or downstream of Akt phosphorylation we examined the effect of HFG-induced apoptosis on the activation state of Akt (Fig. 7*D*). Activated pAkt inhibits apoptosis by inactivating downstream proapoptotic targets (14). Control INS1 cells exposed to HFG, but not HG or HF, showed a marked decrease in the amount of pAkt (Ser 473), consistent with their progression through apoptosis. *Fis1* RNAi–expressing cells also exhibited a dramatic decrease in pAkt because Akt signaling in apoptosis is primarily upstream of the mitochondrial machinery and Fis1 action (27). Expression levels of Akt remained unchanged in both empty vector and *Fis1* RNAi–expressing cells under basal, HG, HF, and HFG culture conditions.

Insulin secretion. Although restoration of mitochondrial fusion improved cell viability under HFG, it did not rescue GSIS (Fig. 7*E*). We found that under HFG, insulin secretion in response to 15 mmol/l glucose is significantly decreased by an average of 31% ($P = 0.023$). Fis1 knockdown cells exposed to similar HFG treatment exhibit the same levels of insulin secretion compared with control cells ($P = 0.43$).

Fis1 expression. Induction of Fis1 expression by HFG was not observed. The relative change in Fis1 expression level after 24-h HFG exposure measured by Western blot yielded results with high variability (SD = 0.552) and insignificant induction compared with control ($n = 3$, $P = 0.97$; data not shown).

DISCUSSION

A number of studies have established that mitochondrial dysfunction plays a role in the development of type 2 diabetes and that exposure of β-cells to high levels of glucose and fatty acids may contribute to the development of the disease (11,28,29). Mitochondrial dysfunction has been observed in the Zucker diabetic fatty rat model. Most notably, superoxide generation is increased and mitochondrial morphologies are short and swollen compared with those of nondiabetic littermates (30). In this article, we report that exposure to toxic nutrient levels induces β-cell mitochondrial fragmentation that is caused by alterations in mitochondrial dynamics. Moreover, preserving mitochondrial dynamics can prevent fragmentation and apoptosis.

Previous studies in a variety of cells have demonstrated the existence of elaborate networks of mitochondria that frequently connect through fusion events. Given the dense appearance of β-cell mitochondria and the relatively short unit size, it was unclear whether fusion and fission occur in β-cells and whether these play any role in the development of diabetes. Here, we demonstrate for the first time that mitochondria in β-cells continuously undergo fusion and fission and that these interactions may function to negate the detrimental effects of long-term exposure to high levels of nutrients. Under normal condition, the dynamic activity of mitochondria is evident in clonal β-cells, dispersed β-cells, and β-cells within an intact islet. Individual whole-cell mitochondrial fusion assays performed within intact islets indicate that fusion rates vary from cell to cell. The intercellular variation appears to be greater between β-cells within an islet compared with

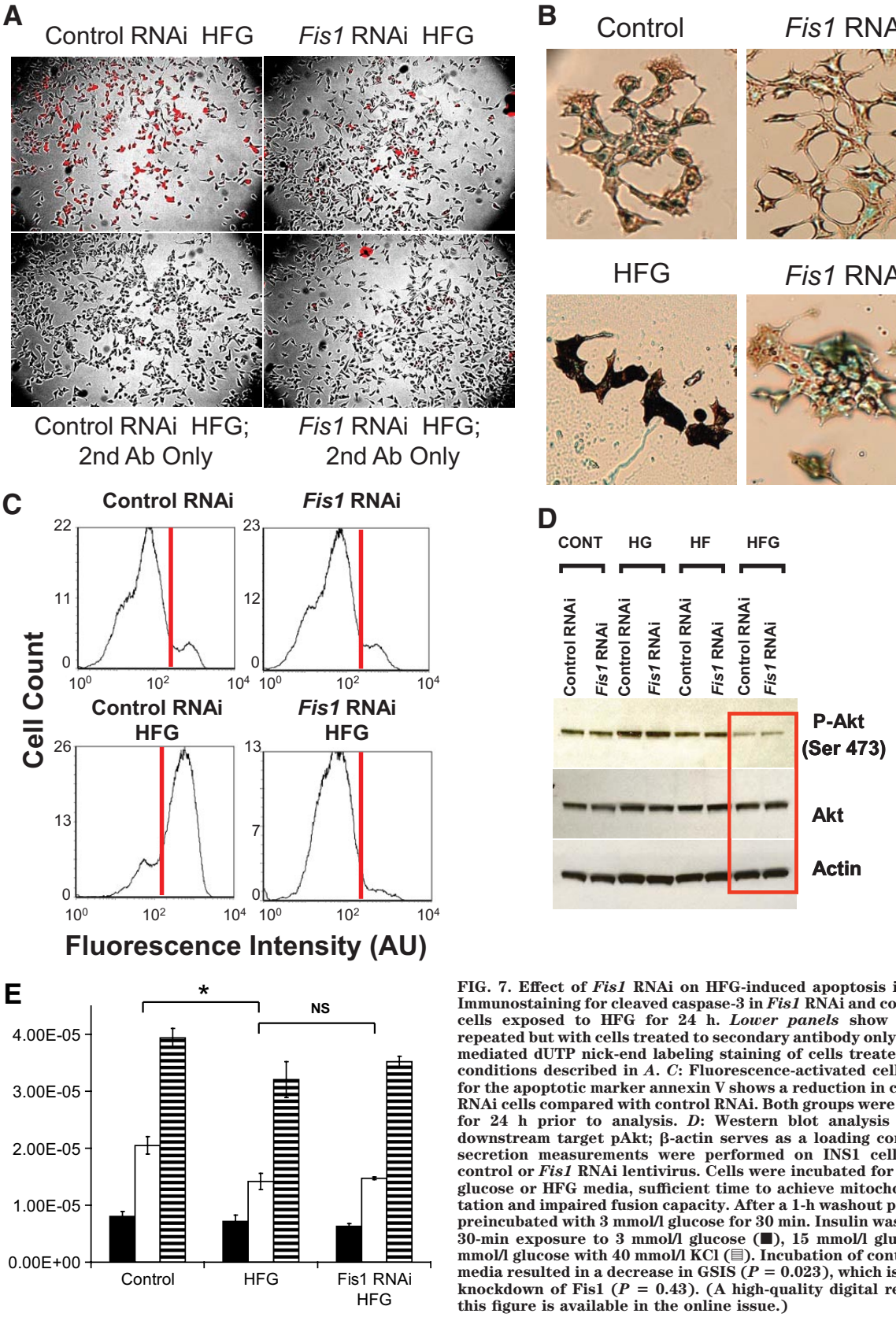

FIG. 7. Effect of *Fis1* RNAi on HFG-induced apoptosis in INS1 cells. *A*: Immunostaining for cleaved caspase-3 in *Fis1* RNAi and control RNAi INS1 cells exposed to HFG for 24 h. *Lower panels* show the experiment repeated but with cells treated to secondary antibody only. *B*: Transferase-mediated dUTP nick-end labeling staining of cells treated with the same conditions described in *A*. *C*: Fluorescence-activated cell sorter analysis for the apoptotic marker annexin V shows a reduction in cell death in *Fis1* RNAi cells compared with control RNAi. Both groups were exposed to HFG for 24 h prior to analysis. *D*: Western blot analysis of Akt and its downstream target pAkt; β-actin serves as a loading control. *E*: Insulin secretion measurements were performed on INS1 cells infected with control or *Fis1* RNAi lentivirus. Cells were incubated for 4 h in 11 mmol/l glucose or HFG media, sufficient time to achieve mitochondrial fragmentation and impaired fusion capacity. After a 1-h washout period, cells were preincubated with 3 mmol/l glucose for 30 min. Insulin was measured after 30-min exposure to 3 mmol/l glucose (■), 15 mmol/l glucose (□), or 15 mmol/l glucose with 40 mmol/l KCl (▤). Incubation of control cells in HFG media resulted in a decrease in GSIS ($P = 0.023$), which is not restored by knockdown of Fis1 ($P = 0.43$). (A high-quality digital representation of this figure is available in the online issue.)

dispersed β-cells. This may correlate to previous studies by Marsh and colleagues suggesting that differences in the level of mitochondrial branching between β-cells in a islet may reflect differences in secretory capacity (31). Indeed, it is conceivable that cells with more branched mitochondrial networks will have a different PAGFPmt fusion rate than cells with less branched mitochondria.

Tagging individual mitochondria with matrix-targeted PAGFPmt enables quantitative dissection of mitochondrial architecture and dynamics. Mitochondria in primary

β-cells are densely packed, which can lead to an overestimation of mitochondrial size and the impression of a continuous structure. However, when the matrix boundaries of each mitochondrial unit are determined by photoactivation of PAGFPmt, it is clear that many of the larger convoluted webs actually represent short strands of mitochondria juxtaposed with one another without matrix continuity. For comparison, COS cells possess very elaborate mitochondrial structures that often appear to be interconnected within a complex web. Despite the appearance of connectivity, the average COS cell mitochondrion is only about 1% of the size of the entire web, which is revealed by PAGFPmt photoactivation of individual units (6). Interestingly, it has been reported that mitochondria are unconnected and can have distinct functional properties (32). With the PAGFPmt-based mitochondrial fusion assays, we have been able to observe that β-cell mitochondria undergo transient fusion events. The relatively small size of these units is not the result of the inability of these mitochondria to undergo fusion. We show that these mitochondria frequently go through fusion, shown by complete equilibration of PAGFPmt throughout the web in as little as 1 h. Compared with other cell types, the time to equilibrium we report is similar to what has been observed in HeLa cells and several other cell types including rat hipoccampal neurons (16).

Interestingly, INS1 cell mitochondria assemble into more elongated and convoluted networks than primary β-cells. Our data suggest that the mechanism underlying differences in mitochondrial morphology between cell types may be related to the levels of OPA1 expression. We report that overexpression of OPA1 leads to the appearance of short punctate mitochondria. Similarly, overexpression of another mitochondrial fusion protein, Mfn2, leads to the clustering of mitochondria into short fragments (33). In INS1 cells, it takes larger increases in OPA1 to achieve similar fragmentation of the mitochondrial network. These findings suggest that INS1 cell mitochondria are able to maintain networking ability when faced with disruptions in the balance between fusion and fission.

Altering mitochondrial fission by expressing DN DRP1 leads to the formation of very elongated mitochondrial tubules along with the appearance of swollen sections. In primary β-cells, expression of DN DRP1 leads to the formation of large swollen mitochondria that likely represent a superfused state. HFG, the synergistic combination of elevated glucose and fatty acid, is an in vitro model of type 2 diabetes described previously (34) and has been shown to cause progressive β-cell dysfunction and cell death (35). Previous studies have shown that HFG leads to an increased level of $\Delta\Psi$mt heterogeneity and the appearance of a growing population of depolarized mitochondria (14). It is conceivable that these changes may be mediated by alterations in mitochondrial dynamics and network morphology. Indeed, we found dramatic differences in mitochondrial morphology between control (basal glucose) and HFG-treated groups. HFG caused the appearance of numerous punctate mitochondria and overall fragmentation of the mitochondrial network. When combined with palmitate, increasing concentrations of glucose (5, 11, and 20 mmol/l) lead to increasing levels of fragmentation in a dose-dependent manner. However, in the absence of palmitate, even 20 mmol/l glucose does not affect mitochondrial architecture. These data are congruent with the synergistic effects of palmitate and glucose that have been reported previously (10).

Interestingly, with higher levels of glucose alone and longer exposure, expression of the mitochondrial fission protein DRP1 is increased (36). This finding supports an important role for mitochondrial fission in apoptosis because the induction of DRP1 expression increased high glucose–induced apoptosis in DRP1 wild-type cells. Cells expressing a DN DRP1 were not affected by the induction of DRP1 expression. Our results indicate that with the combination of high fat and glucose, mitochondrial fragmentation occurs within 4 h. Furthermore, we report that alterations in mitochondrial fusion mediate mitochondrial fragmentation, whereas DRP1 translocation is unaffected. Rescue of mitochondrial fusion ability was sufficient to prevent HFG-induced apoptosis.

Fragmentation of the mitochondrial network may be mediated by increased fission, decreased fusion, or conditions characterized by uniquely high expression levels of fusion proteins such as OPA1 or Mfn2. To determine which of these possibilities occurs under HFG, we quantified mitochondrial dynamics by studying the spread of photoconverted PAGFPmt across the mitochondrial web. We found significant abrogation of mitochondrial fusion in cells exposed to HFG compared with control (basal glucose). The disruption of mitochondrial dynamics in the presence of palmitate appears at 11 mmol/l glucose but is not apparent at 5 mmol/l glucose. As shown in the mitochondrial morphometry analysis, after 24-h HFG, there remains a small population of mitochondria that retains a relatively elongated morphology. Indeed, certain cells retain complex mitochondrial morphology that is comprised of a mixture of elongated and punctuate structures. This may represent an intermediate stage prior to full fragmentation. Future work will address whether these cells represent a population that is less susceptible to apoptosis. Cells under HFG that do not exhibit mitochondrial fragmentation are still capable of mitochondrial fusion, shown by PAGFPmt dilution (see supplemental material). However, the kinetics of PAGFPmt sharing in these cells is reduced compared with control cells, indicating that fusion activity is compromised even before fragmentation is apparent.

The contribution of fission machinery to fragmentation was determined by analyzing the effect of HFG on Fis1 and DRP1. Analysis of Fis1 transcript as well as protein levels in cells treated with HFG did not reveal a statistically significant induction of this protein. Although expression does not change, we show that HFG is accompanied by recruitment of DRP1 to mitochondrial fission sites. This was inhibited in cells treated with *Fis1* RNAi, indicating an essential role for Fis1. We rationalized that the inhibition of fission may balance reduced fusion activity observed under HFG. Indeed, *Fis1* RNAi restored mitochondrial dynamics and morphology in HFG-treated cells, determined by the spreading and dilution of matrix PAGFPmt through the mitochondrial network.

In our studies, knockdown of the fission protein Fis1 did not result in robust morphological changes in INS1 cells (37). This finding suggests that INS1 cells are able to counteract the effects of reduced fission by balancing the rate of fusion. Indeed, our data indicate that Fis1 knockdown is accompanied by a reduction in the fusion rate reported by the PAGFPmt dilution assay. Because fusion and fission events are paired, it is conceivable that decreased fission activity may render the mitochondrial webs more static, suggesting that a certain level of fission is required for an optimal mitochondrial dynamics rate.

Additionally, the lack of change in gross mitochondrial morphology with Fis1 knockdown may be due to the packed and entangled appearance of mitochondria in INS1 cells compared with other cell types such as fibroblasts. The density of mitochondria leads to a large percentage of juxtaposed mitochondria that are not necessarily fused. Under these conditions, alterations in the level of connectivity can produce a measurable shift in PAGFPmt dilution without necessarily altering the overall morphology.

The mechanism by which HFG leads to mitochondrial fragmentation may be related to an increase in ROS. HFG has been shown to increase superoxide levels (38). In a separate study, treatment of INS1 with H_2O_2 resulted in fragmentation of the mitochondrial network, suggesting that nutrient-induced ROS production can lead to mitochondrial fragmentation (39). On the other hand, other studies have shown that dynamic changes in mitochondrial morphology may influence glucose-induced overproduction of ROS (7). In H9C2 and CRL-1439 cell lines, inhibition of mitochondrial fission with DN DRP1 attenuates ROS production and mitochondrial fragmentation induced by acute exposure to 50 mmol/l glucose. In neurons, inhibition of fission was found to mitigate NO-induced mitochondrial fragmentation and cell death (40). Thus, it is conceivable that the effect of HFG on mitochondrial morphology may be due to increased ROS damage. The decrease in ROS production in *Fis1* RNAi cells under HFG may be at least partially responsible for the protection from fragmentation and apoptosis. In a previous study, we demonstrate that Fis1 knockdown does not lower ROS levels in INS1 cells under growth conditions. However, a significant decrease was observed in INS1 cells incubated in 22 mmol/l glucose (17).

Inhibition of mitochondrial fission through *Fis1* RNAi markedly reduced apoptosis compared with cells infected with control virus. This result demonstrates the importance of mitochondrial networking in β-cell physiology because preventing HFG-induced fragmentation through *Fis1* RNAi reduces β-cell apoptosis. However, this does not indicate that fragmentation necessarily leads to apoptosis. Indeed, it has been shown that overexpression of hFis1 in INS1 cells only leads to nominal levels of apoptosis. Moreover, fragmentation caused by the expression of DN Mfn1 does not result in apoptosis in INS1 cells (41). Although it is possible to induce fragmentation and apoptosis by Fis1 overexpression in other cell types, it is also possible to prevent apoptosis without affecting mitochondrial fragmentation, which has been demonstrated with the overexpression of Bcl-X_L (42).

Previous studies have raised a number of potential mechanisms by which inhibition of mitochondrial fragmentation can affect apoptosis (43,44). Fragmentation occurs early in the cell death pathway (43,45) and is thought to contribute to the release of cytochrome C into the cytosol, culminating in caspase-mediated apoptosis (45). It is notable that although a decrease in the translocation of BAX to mitochondria and the subsequent release of cytochrome C have been reported with Fis1 knockdown, DN DRP1 left BAX translocation unaffected (46). An article by Martinou and colleagues (47) has shown that inhibition of fission machinery can prevent mitochondrial fragmentation and reduce cytochrome C release. However, Bax/Bak-mediated apoptosis still occurs along with the release of Smac/DIABLO. A more recent article by Bossy-Wetzel and colleagues (48) has reported that mitochondrial fission occurs upstream of BAX translocation. Revealing the relevance and timing of these events in HFG-induced apoptosis in β-cells is a topic for future investigation.

Activated Akt provides protection from apoptosis through phosphorylation and inhibition of proapoptotic proteins such as BAD (24,49). Previous studies have indicated that β-cell survival under elevated glucose or fatty acid is dependent on Akt phosphorylation and that reduced level of pAkt is associated with β-cell loss (24–26). Interestingly, in HFG-treated cells where Fis1 has been knocked down, reduced pAkt was not accompanied by cell death. β-Cell survival enhanced by Fis1 knockdown indicates that the effect of Fis1 occurs downstream of the Akt signaling pathway and that the reduction in mitochondrial fragmentation bypasses the reduction in Akt activity. Recent studies have also indicated that increased calcium influx plays a role in palmitate-mediated β-cell apoptosis (50). Activation of calcineurin by calcium may regulate mitochondrial morphology by dephosphorylation of DRP1 (51,52). However, our results indicate that HFG-mediated mitochondrial fragmentation is not accompanied by an increased level of DRP1 assembly on mitochondria and increased fission but rather a decrease in the level of fusion activity, demonstrated by mtPAGFP diffusion assays.

The role of mitochondrial dynamics in insulin secretion remains unclear. Our data indicate mitochondrial fusion rate is unchanged by acute stimulation by 15 mmol/l glucose. In addition, Fis1-mediated rescue from HFG is not accompanied by improvements in GSIS. Previous studies by our group and by Wollheim and colleagues indicate that altering mitochondrial dynamics proteins Mfn1 and Fis1 does not improve GSIS (17,41,53). It is interesting to note that both Fis1 overexpression and Fis1 knockdown lead to a decrease in GSIS. Together, these data suggest that any disturbance in the balance of fusion and fission can lead to β-cell dysfunction.

ACKNOWLEDGMENTS

This work was supported by National Institutes of Health Grants R01HL071629-03 (to O.S.S.), R01DK074778 (to O.S.S.), and 5T32DK007201 (to A.J.A.M.).

No potential conflicts of interest relevant to this article were reported.

We thank Drs. Alenka Lovy-Wheeler, F. Rob Jackson, and Louis Kerr for help with imaging technologies. We thank Drs. Dani Dagan, Richard Cohen, Gyorgy Hajnoczky, Nika Danial, Jude Deeney, Gordon Yaney, Keith Tornheim, and Sarah Haigh Molina for helpful discussions and comments. We are grateful to the Sixten Gemzéus foundation for supporting J.D.W. with a fellowship.

REFERENCES

1. Skulachev VP. Mitochondrial filaments and clusters as intracellular power-transmitting cables. Trends Biochem Sci 2001;26:23–29
2. Frank S. Dysregulation of mitochondrial fusion and fission: an emerging concept in neurodegeneration. Acta Neuropathol (Berl) 2006;111:93–100
3. Nakada K, Inoue K, Ono T, Isobe K, Ogura A, Goto YI, Nonaka I, Hayashi JI. Inter-mitochondrial complementation: mitochondria-specific system preventing mice from expression of disease phenotypes by mutant mtDNA. Nat Med 2001;7:934–940
4. Arimura S, Yamamoto J, Aida GP, Nakazono M, Tsutsumi N. Frequent fusion and fission of plant mitochondria with unequal nucleoid distribution. Proc Natl Acad Sci U S A 2004;101:7805–7808
5. Chen H, Chomyn A, Chan DC. Disruption of fusion results in mitochondrial heterogeneity and dysfunction. J Biol Chem 2005;280:26185–26192
6. Twig G, Graf SA, Wikstrom JD, Mohamed H, Haigh SE, Elorza A, Deutsch

M, Zurgil N, Reynolds N, Shirihai OS. Tagging and tracking individual networks within a complex mitochondrial web with photoactivatable GFP. Am J Physiol Cell Physiol 2006;291:C176–C184
7. Yu T, Robotham JL, Yoon Y. Increased production of reactive oxygen species in hyperglycemic conditions requires dynamic change of mitochondrial morphology. Proc Natl Acad Sci U S A 2006;103:2653–2658
8. Frieden M, James D, Castelbou C, Danckaert A, Martinou JC, Demaurex N. Ca(2+) homeostasis during mitochondrial fragmentation and perinuclear clustering induced by hFis1. J Biol Chem 2004;279:22704–22714
9. Szabadkai G, Simoni AM, Chami M, Wieckowski MR, Youle RJ, Rizzuto R. Drp-1-dependent division of the mitochondrial network blocks intraorganellar Ca2+ waves and protects against Ca2+-mediated apoptosis. Mol Cell 2004;16:59–68
10. El Assaad W, Buteau J, Peyot ML, Nolan C, Roduit R, Hardy S, Joly E, Dbaibo G, Rosenberg L, Prentki M. Saturated fatty acids synergize with elevated glucose to cause pancreatic beta-cell death. Endocrinology 2003; 144:4154–4163
11. Poitout V. Glucolipotoxicity of the pancreatic beta-cell: myth or reality? Biochem Soc Trans 2008;36:901–904
12. Hagman DK, Latour MG, Chakrabarti SK, Fontes G, Amyot J, Tremblay C, Semache M, Lausier JA, Roskens V, Mirmira RG, Jetton TL, Poitout V. Cyclical and alternating infusions of glucose and intralipid in rats inhibit insulin gene expression and Pdx-1 binding in islets. Diabetes 2008;57:424–431
13. Robertson RP. Oxidative stress and impaired insulin secretion in type 2 diabetes. Curr Opin Pharmacol 2006;6:615–619
14. Wikstrom JD, Katzman SM, Mohamed H, Twig G, Graf SA, Heart E, Molina AJ, Corkey BE, de Vargas LM, Danial NN, Collins S, Shirihai OS. β-Cell mitochondria exhibit membrane potential heterogeneity that can be altered by stimulatory or toxic fuel levels. Diabetes 2007;56:2569–2578
15. Kuznetsov AV, Usson Y, Leverve X, Margreiter R. Subcellular heterogeneity of mitochondrial function and dysfunction: evidence obtained by confocal imaging. Mol Cell Biochem 2004;256–257:359–365
16. Karbowski M, Arnoult D, Chen H, Chan DC, Smith CL, Youle RJ. Quantitation of mitochondrial dynamics by photolabeling of individual organelles shows that mitochondrial fusion is blocked during the Bax activation phase of apoptosis. J Cell Biol 2004;164:493–499
17. Twig G, Elorza A, Molina AJ, Mohamed H, Wikstrom JD, Walzer G, Stiles L, Haigh SE, Katz S, Las G, Alroy J, Wu M, Py BF, Yuan J, Deeney JT, Corkey BE, Shirihai OS. Fission and selective fusion govern mitochondrial segregation and elimination by autophagy. EMBO J 2008;27:433–446
18. Stojanovski D, Koutsopoulos OS, Okamoto K, Ryan MT. Levels of human Fis1 at the mitochondrial outer membrane regulate mitochondrial morphology. J Cell Sci 2004;117:1201–1210
19. Stojanovski D, Koutsopoulos OS, Okamoto K, Ryan MT. Levels of human Fis1 at the mitochondrial outer membrane regulate mitochondrial morphology. J Cell Sci 2004;117:1201–1210
20. Arai R, Ito K, Wakiyama M, Matsumoto E, Sakamoto A, Etou Y, Otsuki M, Inoue M, Hayashizaki Y, Miyagishi M, Taira K, Shirouzu M, Yokoyama S. Establishment of stable hFis1 knockdown cells with an siRNA expression vector. J Biochem 2004;136:421–425
21. Bowes T, Gupta RS. Novel mitochondrial extensions provide evidence for a link between microtubule-directed movement and mitochondrial fission. Biochem Biophys Res Commun 2008;376:40–45
22. Downward J. PI 3-kinase, Akt and cell survival. Semin Cell Dev Biol 2004;15:177–182
23. Jetton TL, Lausier J, LaRock K, Trotman WE, Larmie B, Habibovic A, Peshavaria M, Leahy JL. Mechanisms of compensatory β-cell growth in insulin-resistant rats: roles of Akt kinase. Diabetes 2005;54:2294–2304
24. Tuttle RL, Gill NS, Pugh W, Lee JP, Koeberlein B, Furth EE, Polonsky KS, Naji A, Birnbaum MJ. Regulation of pancreatic beta-cell growth and survival by the serine/threonine protein kinase Akt1/PKBalpha. Nat Med 2001;7:1133–1137
25. Wrede CE, Dickson LM, Lingohr MK, Briaud I, Rhodes CJ. Protein kinase B/Akt prevents fatty acid-induced apoptosis in pancreatic beta-cells (INS-1). J Biol Chem 2002;277:49676–49684
26. Srinivasan S, Bernal-Mizrachi E, Ohsugi M, Permutt MA. Glucose promotes pancreatic islet beta-cell survival through a PI 3-kinase/Akt-signaling pathway. Am J Physiol Endocrinol Metab 2002;283:E784–E793
27. Danial NN, Korsmeyer SJ. Cell death: critical control points. Cell 2004;116: 205–219
28. Lowell BB, Shulman GI. Mitochondrial dysfunction and type 2 diabetes. Science 2005;307:384–387
29. Maechler P, Wollheim CB. Mitochondrial function in normal and diabetic beta-cells. Nature 2001;414:807–812
30. Bindokas VP, Kuznetsov A, Sreenan S, Polonsky KS, Roe MW, Philipson LH. Visualizing superoxide production in normal and diabetic rat islets of Langerhans. J Biol Chem 2003;278:9796–9801
31. Noske AB, Costin AJ, Morgan GP, Marsh BJ. Expedited approaches to whole cell electron tomography and organelle mark-up in situ in high-pressure frozen pancreatic islets. J Struct Biol 2008;161:298–313
32. Collins TJ, Berridge MJ, Lipp P, Bootman MD. Mitochondria are morphologically and functionally heterogeneous within cells. EMBO J 2002;21: 1616–1627
33. Huang P, Yu T, Yoon Y. Mitochondrial clustering induced by overexpression of the mitochondrial fusion protein Mfn2 causes mitochondrial dysfunction and cell death. Eur J Cell Biol 20007;86:289–302
34. Roduit R, Morin J, Masse F, Segall L, Roche E, Newgard CB, Assimacopoulos-Jeannet F, Prentki M. Glucose down-regulates the expression of the peroxisome proliferator-activated receptor-alpha gene in the pancreatic beta-cell. J Biol Chem 2000;275:35799–35806
35. Poitout V, Robertson RP. Minireview: secondary beta-cell failure in type 2 diabetes–a convergence of glucotoxicity and lipotoxicity. Endocrinology 2002;143:339–342
36. Men X, Wang H, Li M, Cai H, Xu S, Zhang W, Xu Y, Ye L, Yang W, Wollheim CB, Lou J. Dynamin-related protein 1 mediates high glucose induced pancreatic beta cell apoptosis. Int J Biochem Cell Biol 2008;41:879–890
37. Rubinson DA, Dillon CP, Kwiatkowski AV, Sievers C, Yang L, Kopinja J, Rooney DL, Zhang M, Ihrig MM, McManus MT, Gertler FB, Scott ML, Van PL. A lentivirus-based system to functionally silence genes in primary mammalian cells, stem cells and transgenic mice by RNA interference. Nat Genet 2003;33:401–406
38. Brownlee M. A radical explanation for glucose-induced beta cell dysfunction. J Clin Invest 2003;112:1788–1790
39. Maechler P, Jornot L, Wollheim CB. Hydrogen peroxide alters mitochondrial activation and insulin secretion in pancreatic beta cells. J Biol Chem 274:27905–27913, 1999
40. Bossy-Wetzel E, Barsoum MJ, Godzik A, Schwarzenbacher R, Lipton SA. Mitochondrial fission in apoptosis, neurodegeneration and aging. Curr Opin Cell Biol 2003;15:706–716
41. Park KS, Wiederkehr A, Kirkpatrick C, Mattenberger Y, Martinou JC, Marchetti P, Demaurex N, Wollheim CB. Selective actions of mitochondrial fission/fusion genes on metabolism-secretion coupling in insulin-releasing cells. J Biol Chem 2008;283:33347–33356
42. James DI, Parone PA, Mattenberger Y, Martinou JC. hFis1, a novel component of the mammalian mitochondrial fission machinery. J Biol Chem 2003;278:36373–36379
43. Frank S, Gaume B, Bergmann-Leitner ES, Leitner WW, Robert EG, Catez F, Smith CL, Youle RJ. The role of dynamin-related protein 1, a mediator of mitochondrial fission, in apoptosis. Dev Cell 2001;1:515–525
44. Olichon A, Baricault L, Gas N, Guillou E, Valette A, Belenguer P, Lenaers G. Loss of OPA1 perturbates the mitochondrial inner membrane structure and integrity, leading to cytochrome c release and apoptosis. J Biol Chem 2003;278:7743–7746
45. Heath-Engel HM, Shore GC. Mitochondrial membrane dynamics, cristae remodelling and apoptosis. Biochim Biophys Acta 2006;1763:549–560
46. Lee YJ, Jeong SY, Karbowski M, Smith CL, Youle RJ. Roles of the mammalian mitochondrial fission and fusion mediators Fis1, Drp1, and Opa1 in apoptosis. Mol Biol Cell 2004;15:5001–5011
47. Parone PA, James DI, Da CS, Mattenberger Y, Donze O, Barja F, Martinou JC. Inhibiting the mitochondrial fission machinery does not prevent Bax/Bak-dependent apoptosis. Mol Cell Biol 2006;26:7397–7408
48. Yuan H, Gerencser AA, Liot G, Lipton SA, Ellisman M, Perkins GA, Bossy-Wetzel E. Mitochondrial fission is an upstream and required event for bax foci formation in response to nitric oxide in cortical neurons. Cell Death Differ 2007;14:462–471
49. Jetton TL, Lausier J, LaRock K, Trotman WE, Larmie B, Habibovic A, Peshavaria M, Leahy JL. Mechanisms of compensatory beta-cell growth in insulin-resistant rats: roles of Akt kinase. Diabetes 2005;54:2294–2304
50. Choi SE, Kim HE, Shin HC, Jang HJ, Lee KW, Kim Y, Kang SS, Chun J, Kang Y. Involvement of Ca2+-mediated apoptotic signals in palmitate-induced MIN6N8a beta cell death. Mol Cell Endocrinol 2007;72:50–62
51. Cribbs JT, Strack S. Reversible phosphorylation of Drp1 by cyclic AMP-dependent protein kinase and calcineurin regulates mitochondrial fission and cell death. EMBO Rep 20007;8:939–944
52. Cereghetti GM, Stangherlin A, Martins de BO, Chang CR, Blackstone C, Bernardi P, Scorrano L. Dephosphorylation by calcineurin regulates translocation of Drp1 to mitochondria. Proc Natl Acad Sci U S A 2008;105: 15803–15808
53. Twig G, Hyde B, Shirihai OS. Mitochondrial fusion, fission and autophagy as a quality control axis: The bioenergetic view. Biochim Biophys Acta 2008;1777:1092–1097